in superconducting junctions offer a novel way of exerting control of the quantum ground state of the system. Varying the position of a domain wall with a realistic magnetization profile taking into account magnetic anisotropy and spin stiffness, we demonstrate that the position of the domain wall controls whether the junction is in a 0- or π-state. In this way, it becomes possible to exert dynamic control over the quantum ground state within a single sample: the motion of the domain wall manipulates the proximity effects responsible for the oscillatory nature of the superconducting order parameter in the ferromagnetic (F) region, as well as the magnetic correlations and destruction of superconductivity in the superconducting (S) layers. Moreover, we will show that the domain wall dynamics can result in an effective superconducting switch, where the system changes from a resistive state to a dissipationless one. We compute the critical temperature of a domain wall nanostructure in the ballistic regime in an entirely self-consistent manner, which is necessary when it is unknown *a priori* what the ground state of the system is. We find suitable spin switch candidates that transition from a superconducting state to a normal one, even at $T = 0$, as the domain wall is shifted. These results show that superconducting spintronics via magnetic domain wall motion can be used not only to change the superconducting quantum state, but even turn superconductivity itself on and off.

We first outline the theoretical framework used in our calculations to compute the superconducting quantum ground state. Next, we present analytical and numerical results for 0-π transitions both in the ballistic and diffusive regime of transport, including the possibility of switching from a resistive to dissipationless state simply by moving the domain wall. We then give a detailed discussion of our results, including candidate materials for the predicted effects, and experimental feasibility of our proposed setup. Finally, we summarize our findings.

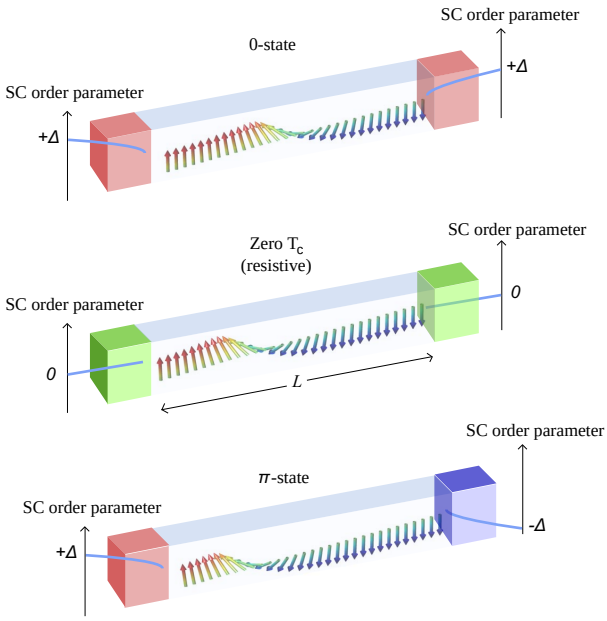

FIG. 1: **Proposed setup**. A magnetic domain wall is present in a ferromagnetic layer of width L, separating two conventional s-wave superconductors. Inducing domain-wall motion to a new position can alter the quantum ground state of the junction, triggering a 0-π transition. Moving the domain-wall changes the critical temperature T_c and may even reduce it to zero (middle figure), thus destroying superconductivity. The domain-wall can be moved via an applied current, external field, or spin-wave excitations to specific locations by artificially tailored pinning sites *e.g.* via geometrical notches in the sample.

Domain walls in Josephson junctions

To model a realistic domain wall, we minimize the free energy functional for an inhomogeneous ferromagnet including exchange stiffness and anisotropy:

$$\mathcal{F} = \int \mathrm{d}x[A(\partial_x \mathbf{M})^2/2 - K_{\text{easy}} M_z^2 + K_{\text{hard}} M_x^2]. \quad (1)$$

Here, A is the exchange stiffness while K_{easy} and K_{hard} are the anisotropy energies associated with the easy and hard axes of the magnetization, $\mathbf{M}$, respectively. The result[26] is $\mathbf{M}(x) = [0, \sin\theta(x), \cos\theta(x)]$ where $\theta(x)$ determines the domain wall profile and is given by:

$$\theta(x) = 2\arctan\{\exp[(x - X)/\lambda]\}, \quad (2)$$

where λ is the domain wall width, determined by A and K_{easy}. We have also introduced the position of the center of the domain wall X, which will play an important role in what follows. With the magnetization texture in hand, we now insert it into the corresponding equations of motion for the Green's function which in turn enables us to compute the supercurrent in the system. In the diffusive regime, we make use of the quasiclassical Usadel equation[27] with the above magnetization profile $\mathbf{M}(x)$:

$$D[\hat{\partial}, \hat{G}[\hat{\partial}, \hat{G}]] + i[\varepsilon\hat{\rho}_3 + \text{diag}[\mathbf{h}\cdot\underline{\sigma}, (\mathbf{h}\cdot\underline{\sigma})^T], \hat{G}] = 0. \quad (3)$$

Here D is the diffusion constant, $\mathbf{h}||\mathbf{M}$ is the exchange field, ε is the quasiparticle energy, $\hat{\partial}$ is the derivative operator, $\hat{G}$ represents the total Green's function and $\hat{\rho}_3$ and $\underline{\sigma}$ are 4×4 and 2×2 Pauli matrixes, respectively. The Usadel equation is supplemented by the Kupriyanov-Lukichev[28] boundary conditions at interfaces along the x-axis;

$$2\zeta\hat{G}\hat{\partial}\hat{G} = [\hat{G}_{\text{BCS}}(\phi), \hat{G}], \quad (4)$$

in which $\hat{G}_{\text{BCS}}$ is the bulk solution and ζ controls the interface opacity. For stability in the numerical computations, we use the so-called Ricatti parametrization[29] of the Green's function. Finally, the supercurrent may be computed according to the formula:

$$I_{\text{super}} = j_0 \int_0^\infty \mathrm{d}\varepsilon\ \mathrm{Tr}\Big\{\hat{\rho}_3\Big(\check{g}\frac{\partial\check{g}}{\partial x}\Big)^K\Big\}. \quad (5)$$

where $j_0 = -N_0|e|D/16$ is a normalization constant where N_0 is the normal-state density of states and e is the electron charge. The key observation is that when the Josephson current I_{super} changes sign, a 0-π transition has taken place.

We now turn to the ballistic regime to investigate the transport and thermodynamic properties of SFS nanojunctions with controllable domain walls. We utilize the microscopic Bogoliubov-de Gennes (BdG) technique[30] which enables us to fully isolate the superconducting pairing correlations in the system and investigate the precise behavior of the proximity-induced supercurrent. In terms of the quasiparticle amplitudes $u_{n\sigma}$ and $v_{n\sigma}$ with excitation energy ϵ_n, and spin σ, the BdG equations are compactly written as,

$$\begin{pmatrix} \mathcal{H}-h_z & -h_x+ih_y & 0 & \Delta \\ -h_x-ih_y & \mathcal{H}+h_z & \Delta & 0 \\ 0 & \Delta^* & -(\mathcal{H}-h_z) & -h_x-ih_y \\ \Delta^* & 0 & -h_x+ih_y & -(\mathcal{H}+h_z) \end{pmatrix} \Psi_n = \epsilon_n \Psi_n, \tag{6}$$

where we define the vector $\Psi_n \equiv (u_{n\uparrow}, u_{n\downarrow}, v_{n\uparrow}, v_{n\downarrow})^T$. The pair potential $\Delta(x)$ must be determined self-consistently by solving the BdG equations together with the condition,

$$\Delta(x) = \frac{g}{2}\sum_n [u_{n\uparrow}(x)v^*_{n\downarrow}(x) + u_{n\downarrow}(x)v^*_{n\uparrow}(x)] \tanh\left(\frac{\epsilon_n}{2T}\right), \tag{7}$$

where the sum is restricted to those quantum states with positive energies below an energy cutoff, specified below. The single particle Hamiltonian $\mathcal{H}$ is expressed as, $\mathcal{H} = 1/(2m)(-\partial_x^2 + k_x^2 + k_y^2) - \mu + U(x)$, where μ is the Fermi energy, and $U(x)$ is the spin-independent interface scattering potential which we take to be of the form $U(x) = U_B[\delta(x + L/2) + \delta(x - L/2)]$, where L is the width of the ferromagnetic region. The terms $1/(2m)(k_x^2 + k_y^2)$ in the Hamiltonian represent the energy of the transverse modes.

To determine the self-consistent ground state of the SFS system, one must calculate the free energy, $\mathcal{F}$, given by,

$$\mathcal{F} = -2T\sum_n \ln\left[2\cosh\left(\frac{\epsilon_n}{2T}\right)\right] + \frac{\langle|\Delta(x)|^2\rangle}{g}, \tag{8}$$

where $\langle\ldots\rangle$ denotes spatially averaging over the entire system, and the pair potential is self consistently calculated in Eq. (7). The supercurrent can be found by taking the derivative of the free energy with respect to the phase difference ϕ: $j_x = 2e(\partial\mathcal{F}/\partial\phi)$. Note that we have not made any assumption of a weak proximity effect in the above - the results are obtained by solving the full proximity effect equations numerically.

Inducing a 0-π transition via domain-wall motion

The underlying physics for this phenomenon may be most easily understood in the limit of a thin domain-wall. In that case, one may think of the ferromagnetic region as an effective bilayer with two ferromagnets in an antiparallel configuration. Whether the junction is in a 0- or π-state is determined by the total phase-shift picked up by an Andreev bound-state carrying the supercurrent through the ferromagnet. This phase-shift depends on the exchange field orientation and the length of the junction. When the ferromagnet consists of two regions with antiparallell magnetization, the phase-shift is partially compensated when the bound-state first propagates through one ferromagnet and then the second one with opposite magnetization direction. In fact, when the layers have exactly the same width, the junction is essentially equivalent to an SNS system[31]. However, if the layers are allowed to have different thicknesses, the phase-shift picked up by the Andreev bound-state will allow for a π-state to be formed as long as h and/or L are sufficiently large to induce a π-phase difference as the bound-state makes a full round-trip between the superconductors. We can then qualitatively understand why moving the domain wall will induce 0-π transitions: the position of the wall determines the effective phase-shift experienced by the Andreev bound-state as it propagates between the superconductors. When the domain wall is thick, the analogy to a bilayer breaks down since the spin-rotation takes place over a much longer distance. In our approach, we have access to an arbitrary domain wall profile and have verified that the domain wall position still determines whether the junction is in a 0- or π-state in the case where the domain wall extends over a large part of the junction.

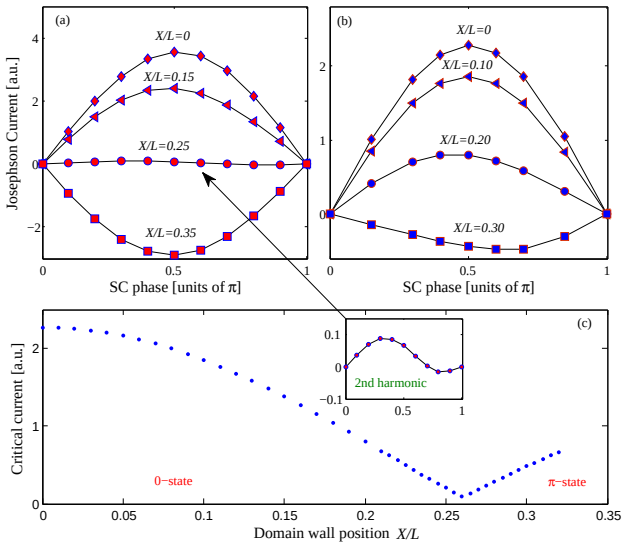

FIG. 2: **Josephson current in the diffusive limit.**. Supercurrent-phase relation for two different parameter sets: (a) $h/\Delta = 5, \lambda/L = 0.02, L/\xi = 1.7$ and (b) $h/\Delta = 8, \lambda/L = 0.05, L/\xi = 1.5$. (c) Critical supercurrent as a function of domain wall position for the same parameter set as in (b). *Inset:* the appearance of a second harmonic in the Josephson relation near the 0-π transition. In all cases, we have used an interface parameter $\zeta = 4$, corresponding to a weakly transparent interface in terms of tunneling, and a temperature $T/T_c = 0.1$.

We start by demonstrating the possibility of having 0-π transitions induced by moving the domain wall in the diffusive regime. In Fig. 2(a) and (b), we have computed the supercurrent-phase relation using two different parameter sets for the sake of showing that this effect does not just occur for special fine-tuned parameters. Fig. 2(c) illustrates the critical current as a function of the domain wall position X in the

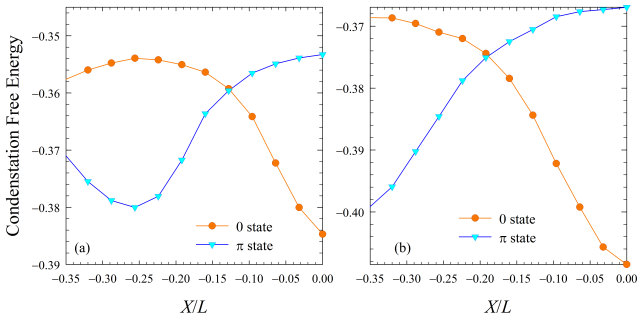

FIG. 3: **Free energy in the ballistic limit**. Control of the quantum state with domain wall motion: (a) depicts the condensation free energy as a function of domain wall motion for both of the self consistently determined π and 0 states. Here $\lambda/L = 0.02$, and $L/\xi = 1.5$. (b) corresponds to $L/\xi = 1$ with all other parameters the same as (a). The center of the junctions corresponds to $X/L = 0$

ferromagnet. In all plots, the transition is clearly seen: the current-phase relation is inverted whereas the critical current decays towards zero and then rises to finite values. We note that our calculation is done for a scenario where the system has relaxed to equilibrium with the domain wall at position X in the junction, thus corresponding to several measurements of the current (yet within one single sample) with the domain wall at rest in different positions. We will later discuss precisely how this may be accomplished experimentally. An alternative measuring scheme would consist of doing measurements on distinct samples with domain walls at pinned, predetermined locations by means of geometrical notches or other sources of pinning potentials in the ferromagnet[36].

For the ballistic results, in all cases we have assumed a superconducting correlation length corresponding to $k_F\xi = 100$ and measure all temperatures in units of T_{c0}, the transition temperature of bulk S material. We consider $T = 0.01$, except when calculating the critical temperature, and fix the energy cutoff at 0.04, in units of μ. Scattering at the interfaces is characterized by parameter $Z_B \equiv mU_B/k_F$, which is unity throughout the calculations unless otherwise noted, corresponding to a moderately transparent interface in terms of tunneling. We have found however that the domain wall position leading to the 0-π transition is weakly dependent on Z_B. This follows from the fact that the magnitude of the exchange interaction h shifts the energy spectrum for spin-up and spin-down quasiparticles by an amount $-h$ and $+h$ respectively. Thus, the oscillatory period of the superconducting correlations in F are primarily determined from the difference of the spin-up and spin-down wavevectors, and not the spin-independent interface scattering.

In the ballistic regime, Fig. 3 demonstrates the thermodynamics of the 0-π transition, which follows from the free energy. We characterize the ground state by finding $\mathcal{F}_S$, the free energy of the whole system in the self consistent state, and $\mathcal{F}_N$, the normal state ($\Delta \equiv 0$) free energy. The normalized condensation free energy is then $\Delta\mathcal{F} \equiv (\mathcal{F}_S - \mathcal{F}_N)/(2E_0)$, where E_0 is the condensation energy of bulk S material at $T = 0$. By comparing the condensation energies of the 0 and

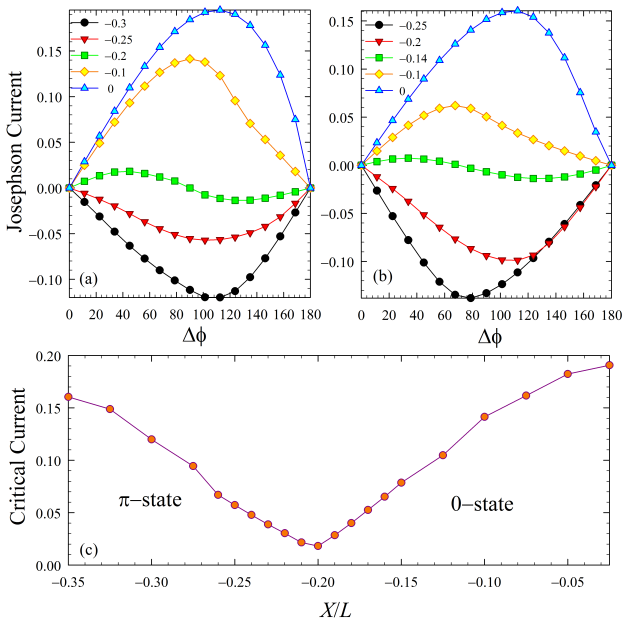

FIG. 4: **Josephson current in the ballistic limit**. Supercurrent-phase relation for two different ferromagnet widths: (a) $h/\Delta = 5, \lambda/L = 0.02, L/\xi = 1$ and (b) $L/\xi = 1.5$. In both cases there is a clear appearance of a second harmonic in the Josephson relation near the 0-π transition. (c) Critical supercurrent as a function of domain wall position for the same F thickness used in (a).

π state configurations as a function of the domain wall position, we can therefore immediately identify the ground state of the system. For both Fig. 3(a) and (b), we see that when the domain wall is located near the center of the ferromagnet ($X = 0$), the 0-state is the ground state. However, when the domain wall is moved closer to the interface, the ground state is the π-state.

Next, in Fig. 4 we examine the charge transport and calculate the Josephson current for the same thicknesses in Fig. 3(a) and (b). The free energy profiles in Fig. 3 revealed that the 0-π crossover occurs at $X/L \approx -0.14$ and $X/L \approx -0.2$ for $L = 1.5\xi$ and $L = \xi$ respectively. This is consistent with the supercurrent behavior of Fig. 4, where for those domain wall positions, the current phase relation acquires additional harmonics at the $0 - \pi$ transition. An experimentally relevant quanitity related to the above results is the critical current. We therefore show in Fig. 4(c) the critical current as a function of domain wall position for the cases considered in (a). This quantity is determined by finding the maximum value of the magnitude of the Josephson current over the entire $\Delta\phi$ interval, for each X. The critical current then has a minimum at the 0-π transition corresponding to the cusp at $X/L \approx -0.2$. Note that the observed behavior is robust in the sense that it is found in both the ballistic and diffusive limit, and for differing thicknesses. This should facilitate making contact with experiment.

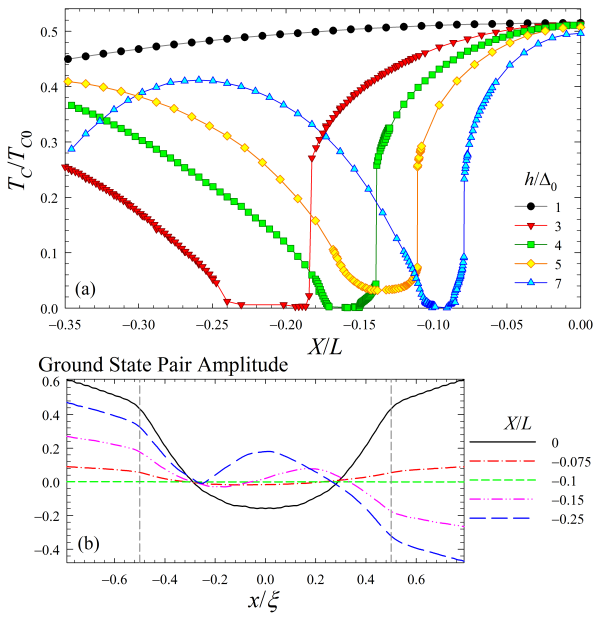

FIG. 5: **Controlling T_c with domain wall motion**. (a) Turning superconductivity on or off: Critical temperature as a function of domain wall position for several different exchange fields (see legend). We assume transparent interfaces and, $\lambda/L = 0.02$, $d_S = 0.95\xi$ and $L/\xi = 1$. In (b) we show the corresponding Cooper pair amplitude for the ground states when $T = 0$ and for an exchange field of $h/\Delta_0 = 7$. Its spatial dependence reveals the transition from the π to 0 state near the minimum of the T_c curve in (a) occurring at $X/L \approx -0.1$, where the system has transitioned to a normal resistive state.

Superconducting on-off switch via domain-wall motion

We next demonstrate that one can obtain a superconducting switch controlled by the position of the domain wall. This effect is revealed in the experimentally relevant critical temperature, which is computed by linearizing the BdG equations (6) near the transition, yielding an eigenvalue problem that is solved using an extension to previous methods.[32] Penetration of the superconducting condensate into the ferromagnet results in the breaking of Cooper pairs by the exchange field and leads to a decrease of the superconducting transition temperature.

We illustrate in Fig. 5(a) the rich variety of switching behavior that can arise when varying the domain wall position. Increasing the exchange field tends to increase the number of T_c oscillations, reflecting the increase in the period of oscillations in the Cooper pairing amplitude that resides in the ferromagnet. The critical temperature is typically indifferent to h near the center of the junction, where the curves coalesce. As the domain wall shifts away from the center, T_c of the system drops abruptly to zero and the system transitions to a normal resistive state in a way that depends strongly on h. This is highly suggestive of a superconducting switch where superconductivity is turned off or on depending on the location of the domain wall. The application of an external field may also introduce additional interesting reentrance effects[33]. It is important to note that this switching effect is not exclusive to Josephson junctions, as we have found that the same effect occurs in a S/F bilayer structure as well.

In analogy with the critical current behavior, the critical temperature contains fingerprints of the $0-\pi$ transition, occurring at around the minimum of the T_c curves. This point is illustrated in Fig. 5(b), where we show the spatial behavior of the Cooper pair amplitude for $h/\Delta_0 = 7$. Five differing domain wall positions are considered: two above and two below $X/L \approx -0.1$, where the system is normal and the pair amplitude vanishes. Clearly, the domain wall position relative to this transition point dictates whether the ground state of the system is the 0 or π state.

Implications for experiments

It is known[22] that domain wall motion may be induced both via application of a current-induced spin-transfer torque and via external magnetic fields[23]. Besides these conventional techniques, another possibility was recently unveiled which might be suitable for our purposes. It was demonstrated in Ref. 24 that domain-wall motion could be obtained via excitation of spin-waves, resulting in a purely magnonic spin-transfer torque. Such spin-waves could be excited via application of a local ac magnetic field $\mathbf{H} = H_0 \sin(\omega t)\hat{z}$, giving rise to domain wall motion toward the spin-wave source. Application of such local fields has been successfully implemented experimentally previously[25], and might be feasible in our setup as well. Current-induced domain wall motion is also an alternative, although it might require an additional polarizing ferromagnetic layer in order to achieve an efficient spin-transfer torque. It has been demonstrated that spin-triplet supercurrents can induce magnetization dynamics[34] and spin-transfer torques[35], and it is thus reasonable to expect that domain wall motion can be induced by a supercurrent spin-transfer torque as well. Once domain wall motion has been induced via *e.g.* one of the above mentioned venues, it is possible to control where the motion terminates, and thus obtain a new ground-state configuration, by artificially tailoring pinning sites which effectively traps the domain wall. This can be accomplished experimentally by *e.g.* making geometrical notches at the desired locations of the ferromagnetic film/wire[36]. Based on the above discussion, there should then be several alternatives available experimentally in order to move the domain wall in the proposed Josephson junction and thus tune the quantum state of the system to either a 0- or π-junction and even turn superconductivity on and off. In terms of candidate materials for observation of the predicted effects, one would need two standard s-wave superconductors, such as Nb or Al, and a magnetic region supporting a domain wall with a width of order $1 - 10$ nm. Such domain walls are known to occur in thin magnetic films Pt/Co/AlO$_x$, Pt(Co/Pt)$_n$, and (Co/Ni)$_n$ (see *e.g.* Ref. 37 for a review). Moreover, although we have in our work considered a Bloch-type of domain wall, we do not expect any qualitative change for Neel or head-to-head domain walls, whose textures may be obtained by a rotation in spin space, since the physical principle remains the same.

This is advantageous in the sense that generic domain walls, as opposed to a specific type of wall texture, will suffice to experimentally observe the influence on superconductivity predicted here.

Conclusion

We have shown that domain wall motion in superconducting junctions provides a unique way to both tune the quantum ground state between $0-$ and $\pi-$phases and also turn on and off superconductivity itself. In particular, we find that the domain wall motion may even trigger a quantum phase transition between a resistive and dissipationless state. Our results point towards new ways to merge superconductivity and spintronics in order to achieve functional properties by utilizing domain wall motion.

Methods

Self-consistent calculation in the ballistic limit. It is convenient numerically to determine the Josephson current using the previously calculated quasiparticle amplitudes and energies. Starting with the quantum mechanical expectation value of the momentum density, we can can express the current j_x in terms of the quasiparticle amplitudes as,

$$j_x = -\frac{ie}{m}\sum_{n,\sigma}\Big[u_{n\sigma}\frac{\partial u^*_{n\sigma}}{\partial x}f_n + v_{n\sigma}\frac{\partial v^*_{n\sigma}}{\partial x}(1-f_n) - c.c.\Big], \qquad (9)$$

where f_n is the Fermi function, $f_n = 1/(\exp(\epsilon_n/(2T))+1)$, and the σ can be either be either spin-up or spin-down ($\uparrow$ or $\downarrow$) relative to the z-quantization axis. Taking the divergence of the current in Eq. (9) and using the BdG equations (6), we find,

$$\frac{\partial j_x}{\partial x} = 2ie\Delta(r)\Big[u^*_{n\uparrow}(x)v_{n\downarrow}(x)f_n - u^*_{n\downarrow}(x)v_{n\uparrow}(x)(1-f_n)\Big] \\ -2ie\Delta^*(r)\Big[u_{n\uparrow}(x)v^*_{n\downarrow}(x)f_n - u_{n\downarrow}(x)v^*_{n\uparrow}(x)(1-f_n)\Big]. \qquad (10)$$

Thus, when the self-consistency condition is satisfied (Eq. (7)), the right hand side vanishes, and the current is conserved. If the self-consistency condition is not strictly satisfied, the terms on the right act effectively as sources of current.

Our numerical procedure for calculating the supercurrent involves first assuming a piecewise constant form for the pair potential in each S layer, Fourier transforming the real-space BdG equations (Eq. (6)), and then diagonalizing the resultant momentum-space matrix. Once the momentum space wavefunctions and energies are found, they are transformed back into real-space and the pair potential is self consistently determined via (7). The newly calculated $\Delta(x)$ is then inserted back into the BdG equations and the above process is repeated. We generally solve $\Delta(x)$ self consistently within about one coherence length of each side of the domain wall/superconductor interface. This leads to the necessary constant current within that region. Deeper within the S regions, we take the self-consistently found $|\Delta(x)|$ and prescribe a phase difference $\Delta\phi$ across both S banks. This provides the necessary source of current, and acts as an effective boundary condition.

[1] Bardeen, J., Cooper, L. N. & Schrieffer, J. R. Microscopic Theory of Superconductivity. *Phys. Rev.* **106**, 162 (1957).

[2] Nelson, K. D., Mao, Z. Q., Maeno, Y. & Liu, Y. Odd-Parity Superconductivity in Sr_2RuO_4, *Science* **306**, 1151 (2004).

[3] Saxena, S. S. *et al.*. Superconductivity at the border of itinerant electron ferromagnetism in UGe_2. *Nature (London)* **406**, 587 (2000).

[4] Aoki, D., Huxley, A., Ressouche, E., Braithwaite, D., Flouquet, J., Brison, J.-P., Lhotel, El. & Paulsen, C. Coexistence of superconductivity and ferromagnetism in URhGe. *Nature (London)* **413**, 613 (2001).

[5] Huy, N. T., Gasparini, A., de Nijs, P. E., Huang, Y., Klaasse, J. C. P., Gortenmulder, T., de Visser, A., Hamann, A., Gorlach, T., & Lohneysen, H. v. Superconductivity on the Border of Weak Itinerant Ferromagnetism in UCoGe. *Phys. Rev. Lett.* **99**, 067006 (2007).

[6] Keizer, R. S., Goennenwein, S. T. B., Klapwijk, T. M., Miao, G., Xiao, G. & Gupta, A. A spin triplet supercurrent through the half-metallic ferromagnet CrO_2. *Nature* **439**, 825 (2006).

[7] Buzdin, A. I. Proximity effects in superconductor-ferromagnet heterostructures. *Rev. Mod. Phys.* **77**, 935 (2005).

[8] Bergeret, F.S., Volkov, A. F. Efetov & K. B. Odd triplet superconductivity and related phenomena in superconductor-ferromagnet structures. *Rev. Mod. Phys.* **77**, 1321 (2005).

[9] Eschrig, M. & Löfwander, T. Triplet supercurrents in clean and disordered half-metallic ferromagnets. *Nature Physics* **4**, 138 (2008).

[10] Tanaka, Y., Golubov, A. A., Kashiwaya, S. & Ueda, M. Anomalous Josephson Effect between Even- and Odd-Frequency Superconductors. *Phys. Rev. Lett.* **99**, 037005 (2007)

[11] Eschrig, M., Löfwander, T., Champel, T., Cuevas, J. C., Kopu, J. & Schön, G. Symmetries of Pairing Correlations in Superconductor-Ferromagnet Nanostructures. *J. Low Temp. Phys.* **147**, 457 (2007).

[12] Bergeret, F. S., Volkov, A. F. & Efetov, K. B. Long-range proximity effects in superconductor-ferromagnet structures. *Phys. Rev. Lett.* **86** 4096 (2001).

[13] Eschrig, M., Kopu, J., Cuevas, J. C. & Schön, G. Theory of Half-Metal/Superconductor Heterostructures. *Phys. Rev. Lett.* **90**, 137003 (2003).

[14] Pajovic, Z., Bozovic, M., Radovic, Z., Cayssol, J. & Buzdin, A. Josephson coupling through ferromagnetic heterojunctions with noncollinear magnetizations. *Phys. Rev. B* **74**, 184509 (2006).

[15] Volkov, A. F., Fominov, Y. V. & Efetov, K. B. Long-range odd triplet superconductivity in superconductor-ferromagnet structures with Neel walls. *Phys. Rev. B* **72**, 184504 (2005).

[16] Linder, J., Yokoyama, T. & Sudbø, A. Theory of superconducting and magnetic proximity effect in S/F structures with inhomogeneous magnetization textures and spin-active interfaces. *Phys. Rev. B* **79**, 054523 (2009).

[17] Halterman, K., Barsic, P. H. & Valls, O. T. Odd Triplet Pairing in Clean Superconductor/Ferromagnet Heterostructures. *Phys. Rev. Lett.* **99**, 127002 (2007).

[18] Anwar, M. S., Czeschka, F., Hesselberth, M., Porcu, M. & Aarts, J. Long-range supercurrents through half-metallic ferromagnetic CrO_2. *Phys. Rev. B* **82**, 100501 (2010).

[19] Robinson, J. W. A., Witt, J. D. S. & Blamire, M. G. Controlled injection of spin-triplet supercurrents into a strong ferromagnet. *Science* **329**, 59 (2010).

[20] Slonczewski, J. C. Current-driven excitation of magnetic multilayers. *J. Magn. Magn. Mater.* **159**, L1 (1996).

[21] Berger, L. Emission of spin waves by a magnetic multilayer traversed by a current. *Phys. Rev. B* **54**, 9353 (1996).

[22] Grollier, J., Chanthbouala, A., Matsumoto, R., Anane, A., Cros, V., Nguyen van Dau, F. & Fert, A. Magnetic domain wall motion via spin transfer *C. R. Physique* **12**, 309 (2011).

[23] Zhu L.Y., Chen T.Y., & Chien C.L., Altering the superconductor transition temperature by domain-wall arrangements in hybrid ferromagnet-superconductor structures. *Phys. Rev. Lett.* **101**, 017004 (2008).
[24] Yan, P., Wang, X. S. & Wang, X. R. All-magnonic spin-transfer torque. *Phys. Rev. Lett.* **107**, 177207 (2011).
[25] Kim, H. K., Hong, S. H., Kim, B. C., Hwang, J. S., Seong, S. M., Park, T. H., Hwang, S. W. & Ahn, D. Generation of Local Magnetic Field by Nano Electro-Magnets. Jpn. J. Appl. Phys. **43**, 2054 (2004).
[26] N. L. Schryer and L. R. Walker, The motion of 180^o domain walls in uniform dc magnetic fields. J. Appl. Phys. 45, 5406 (1974).
[27] Usadel, K. Generalized Diffusion Equation for Superconducting Alloys. *Phys. Rev. Lett.* **25**, 507 (1970).
[28] Kuprianov, M. Y. & Lukichev, V. F. *Sov. Phys. JETP* **67**, 1163 (1988).
[29] Schopohl, N. & Maki, K. Quasiparticle spectrum around a vortex line in a d-wave superconductor. *Phys. Rev.* B **52**, 490 (1995).
[30] de Gennes, P. G. Superconductivity of Metals and Alloys (Addison-Wesley, Reading, Massachusetts, 1989).
[31] Blanter, Y. M. & Hekking, F. W. J. Supercurrent in long SFFS junctions with antiparallel domain configuration. *Phys. Rev. B* **69**, 024525 (2004).
[32] Zhu, J., Krivorotov, I. N., Halterman, K. & Valls, O. T. Angular Dependence of the Superconducting Transition Temperature in Ferromagnet-Superconductor-Ferromagnet Trilayers. *Phys. Rev. Lett.* **105**, 207002 (2010).
[33] Z. Yang, M. Lange, A. Volodin, R. Szymczak & V. V. Moshchalkov, Domain-wall superconductivity in superconductor-ferromagnet hybrids *Nature Mater.* **3**, 793 (2004).
[34] Linder, J. & Yokoyama, T. Supercurrent-induced magnetization dynamics. *Phys. Rev. B* **83**, 012501 (2011).
[35] Zhao, E. & Sauls, J. A. Theory of Nonequilibrium Spin Transport and Spin Transfer Torque in Superconducting-Ferromagnetic Nanostructures. *Phys. Rev. B* **78**, 174511 (2008).
[36] Himeno, A., Ono, T., Nasu, S., Shigeto, K., Mibu, K. & Shinjo, T. Dynamics of a magnetic domain wall in magnetic wires with an artificial neck. *J. Appl. Phys.* 93, 8430 (2003).
[37] Boulle, O., Malinowski, G. & Kläui, M. Current-induced domain wall motion in nanoscale ferromagnetic elements. *Materials Science and Engineering R Reports* **72**, 159 (2011).

Acknowledgments

J.L was supported by the Research Council of Norway, Grant No. 205591/F20 (FRINAT). K.H was supported in part by a grant of HPC resources and the ILIR program sponsored by ONR.

Author contributions

J.L. and K.H. contributed to the formulation of the problem, theoretical calculations, and the preparation of the manuscript.

Additional information

Correspondence and requests for materials may be addressed to J.L. or K.H.

Competing financial interests

The authors declare no competing financial interests.